

Supplementary Information:

Impurity-Driven Formation of Branched Pores in Porous Anodic Alumina

Byeol Kim,^{a,‡} Yong Youn,^{b,‡} Yi-Seul Park,^a Dal Nim Moon,^a Kyungtae Kang,^c Seungwu Han,^b Jin Seok Lee^{a,*}

^aDepartment of Chemistry, Sookmyung Women's University, Seoul 140-742, Korea

^bDepartment of Materials Science and Engineering and Research Institute of Advanced Materials, Seoul National University, Seoul 151-755, Korea

^cDepartment of Applied Chemistry, Kyung Hee University, Yongin, Gyeonggi 446-701, Korea

*To whom correspondence should be addressed. E-mail: jinslee@sookmyung.ac.kr

CONTENTS

- **Experimental Details**
- **Fig. S1.** Characteristic parameters of the porous anodic alumina anodized in a two-step process in 0.3 M oxalic acid at a temperature of 10 °C and a voltage of 40 V for 3 h using Al foils of different purity: (a) defect (%), (b) pore diameter, and (c) film thickness.
- **Fig. S2.** (a) Top-view SEM image of porous anodic alumina anodized in a two-step process (0.3 M oxalic acid at 10 °C and 40 V for 3 h) using Al_{99.0}; (b) EDX analysis of the impurity composition in white squared area of (a); red = Al, green = O, and violet = Si.
- **Fig. S3.** (a) Top-view and cross-section schematic illustration of the geometric parameter of the pore channel. Side view SEM images of porous anodic alumina anodized in a two-step process (0.3 M oxalic acid at 10 °C and 40 V for 3 h) using Al foils of different purity. The geometric parameters employed in the simulation are the following: outer radius (R), inner radius (r), and the angle (θ) from the pore axis to the ridge-top. (b) Anodized Al_{99.999}; $R = 59$ nm, $r = 18$ nm, $\theta = 45^\circ$. (c) Anodized Al_{99.5}; $R = 65$ nm, $r = 23$ nm, $\theta = 46^\circ$. (d) Anodized Al_{99.0}; $R = 64$ nm, $r = 18$ nm, $\theta = 44^\circ$.
- **Fig. S4.** SEM images of porous anodic alumina anodized in a two-step process (0.3 M oxalic acid at 10 °C for 1 h) using Al foils of different purity: (a), (d) 99.999%, (b), (e) 99.5%, and (c), (f) 99.0% at applied voltages of (a)–(c) 30 V, and (d)–(f) 50 V.

Experimental Details

Materials: Three aluminum (Al) foils with different purities (99.999% (containing 0.3 Cu, 0.3 Fe, 1.2 Si, 0.8 Mg (ppm)), 99.5% (containing < 500 Cu, < 4000 Fe, < 3000 Si, < 1000 Zn (ppm)), 99.0% (containing < 1000 Cu, < 7000 Fe, < 5000 Si, < 1000 Zn (ppm))) were supplied by Goodfellow. Each of the foils had a distinct component ratio of impurities containing Cu, Fe, Si and Mg. Oxalic acid ($C_2H_2O_4$), perchloric acid ($HClO_4$), ethanol (C_2H_5OH), phosphoric acid (H_3PO_4), and chromium trioxide (CrO_3) were used. Ultrapure water (Milipore) was used for preparing all the solutions used in this study.

Fabrications of porous anodic alumina: The Al foils were degreased in acetone and washed in deionized water. Then, the foils were electrochemically polished in a mixture of perchloric acid ($HClO_4$) and ethyl alcohol (C_2H_5OH) (1: 4 in volume ratio) at constant potential of 10 V to diminish the roughness of the aluminum surface. The samples were anodized in a 0.3 M oxalic acid solution at 40 V, at constant temperature of 10 °C. After anodization, the alumina film was chemically removed by a mixture of 6 wt% H_3PO_4 and 1.8 wt% CrO_3 at 50 °C for 30 min. The second anodization was carried out under the initial condition. Formed pores were opened in a same mixture of etching solution at 30 °C for 10 min. A double walled bath system with a circulating refrigerant maintaining constant electrolyte temperature was employed, and a carbon electrode was used as the counter electrode for the electrochemical reaction.

Characterization: The morphology and the pore characteristics of the porous alumina films were examined using a field emission scanning electron microscope (FE-SEM) after coating the samples with platinum. Energy dispersive X-ray spectroscopy (EDX) analysis was performed to evaluate the impurities in the anodic alumina film.

Simulation modelling: The electric field distribution was simulated by a steady-state current continuity equation using COMSOL Multiphysics software. The electric potential and electric field distribution in the film need to be solved by the ionic current model since the Al^{3+} and O^{2-} ions migrate through the oxide in the strong electric field. For one-dimensional film geometry, the current density (J) in the oxide changes exponentially depending on the electric field (ϕ), i.e.,

$$J = -2 \frac{\nabla \phi}{|\nabla \phi|} J_0 \sinh(B |\nabla \phi|)$$

,where J_0 and B are constants depending on the material for given temperature. The shape of the oxide in the film resembles a test tube, with a uniform circular cross-section. The geometric domain in the simulation was confined to the oxide layer by neglecting the potential drop in the solution. The shape of the oxide was characterized by the inner radius (oxide-solution interface), outer radius (metal-oxide interface) and the angle from the pore axis to the ridge-top, which were determined by the experimental results (Fig. S3 in the supplementary information). Since we neglected the voltage drop in the solution, the potential at the interface between the oxide and the solution was zero. The potential at the oxide-metal interface was set to the applied anodizing potential. We assumed that the shape of an impurity in the film was circular and that the impurity was difficult to ionize in the oxide layer, and did not migrate freely through the oxide layer.

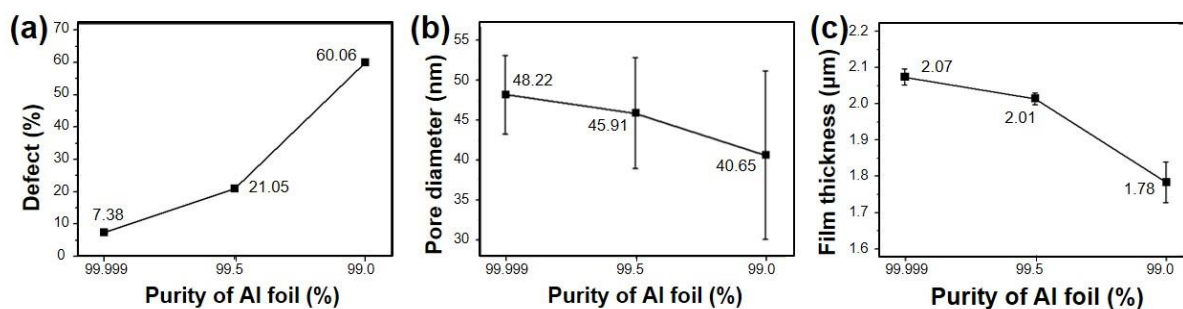


Fig. S1. Characteristic parameters of the porous anodic alumina anodized in a two-step process in 0.3 M oxalic acid at a temperature of 10 °C and a voltage of 40 V for 3 h using Al foils of different purity: (a) defect (%), (b) pore diameter, and (c) film thickness.

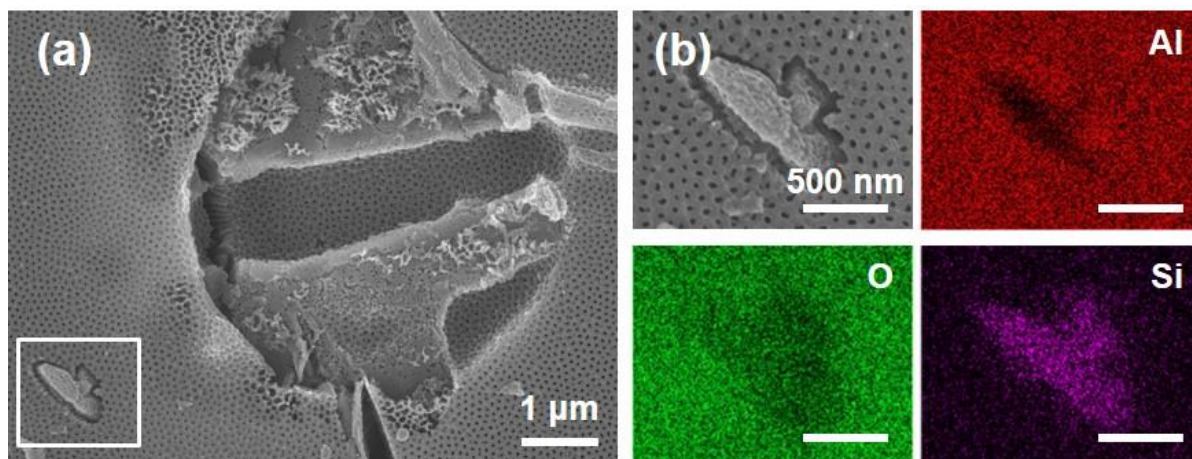


Fig. S2. (a) Top-view SEM image of porous anodic alumina anodized in a two-step process (0.3 M oxalic acid at 10 °C and 40 V for 3 h) using Al_{99.0}; (b) EDX analysis of the impurity composition in white squared area of (a); red = Al, green = O, and violet = Si.

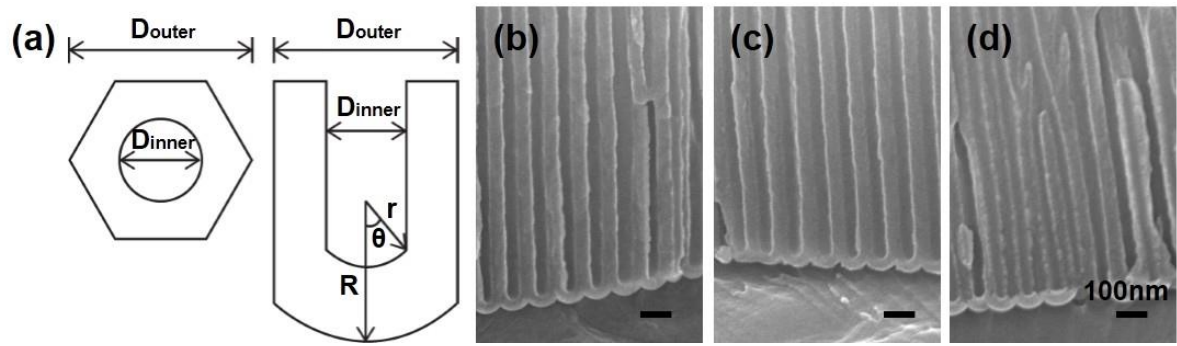


Fig. S3. (a) Top-view and cross-section schematic illustration of the geometric parameter of the pore channel. Side view SEM images of porous anodic alumina anodized in a two-step process (0.3 M oxalic acid at 10 °C and 40 V for 3 h) using Al foils of different purity. The geometric parameters employed in the simulation are the following: outer radius (R), inner radius (r), and the angle (θ) from the pore axis to the ridge-top. (b) Anodized Al_{99.999}; $R = 59$ nm, $r = 18$ nm, $\theta = 45^\circ$. (c) Anodized Al_{99.5}; $R = 65$ nm, $r = 23$ nm, $\theta = 46^\circ$. (d) Anodized Al_{99.0}; $R = 64$ nm, $r = 18$ nm, $\theta = 44^\circ$.

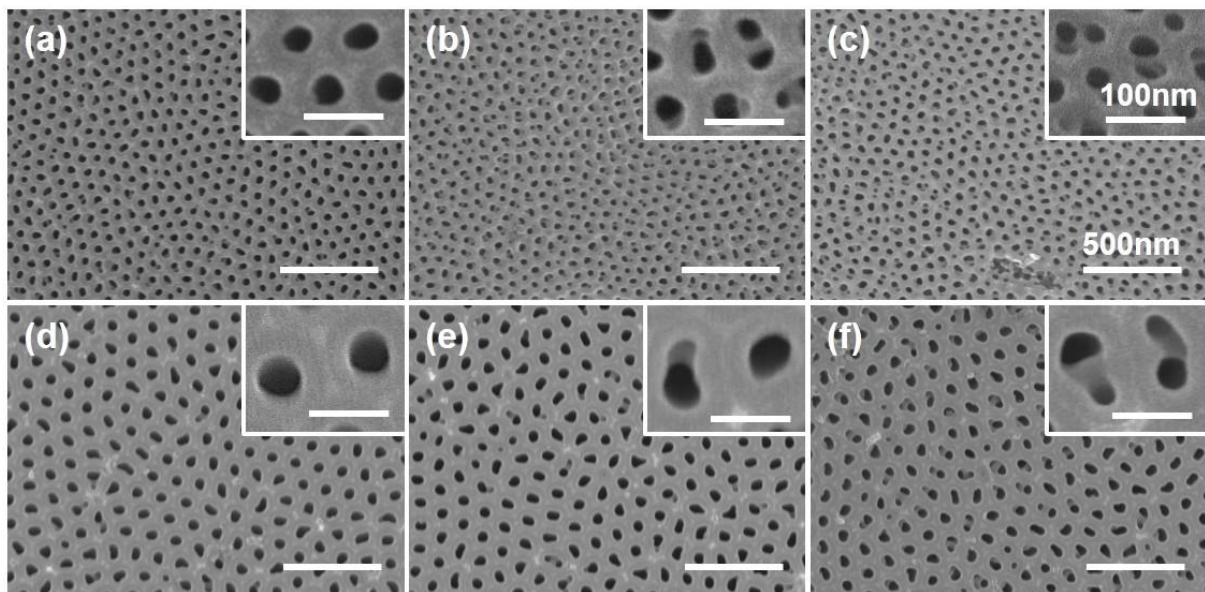


Fig. S4. SEM images of porous anodic alumina anodized in a two-step process (0.3 M oxalic acid at 10 °C for 1 h) using Al foils of different purity: (a), (d) 99.999%, (b), (e) 99.5%, and (c), (f) 99.0% at applied voltages of (a)–(c) 30 V, and (d)–(f) 50 V.